Nanostructure Analysis for Microwave Absorption Properties of Fe_3O_4 Particles by Symmetry Top Rotational Molecular Model

Y. P. Hardianto[1], A. Taufiq[1], A. Hidayat[1], S. Sunaryono[1], A. Listanti[1] and H. Wisodo[1]

[1]Department of Physics, Faculty of Mathematics and Natural Sciences, Universitas Negeri Malang, Jalan Semarang No 5, Malang 65145, Indonesia

Email: ahmad.taufiq.fmipa@um.ac.id

Abstract: In the last years, magnetite (Fe_3O_4) nanoparticles have been prepared with various methods to produce the Fe_3O_4 with high performance especially in microwave absorption properties. In general, the characterization of reflection loss using microwave of the Fe_3O_4 particles has been carried out in the range of 2-18 GHz. In this work, the rotational molecular model was developed to analyze the reflection loss peaks in the range of the frequency. The primary technique of simulation was an interpolation of peak frequencies originating from the molecular rotational transition of the Fe_3O_4 particles. The data analysis presented that the mechanism occurs at the electromagnetic absorption of the Fe_3O_4 particles is rotational molecular. Interestingly, it is presented that the result of the simulation is in line with the results of the characterizations of several materials that have been reported in some literature.

Keywords: Magnetite, reflection loss, microwave absorption, rotational molecular model.

1. Introduction

In the last decades, the research by focusing on the microwave absorption properties of materials has been developed significantly [1]. One of the bases that trigger such development is related to the various applications such as defense technology, especially for radar absorbing material [2]. Nowadays, one of the magnetic material groups that has excellent performance as the radar absorbing material is magnetite (Fe_3O_4) nanoparticles [3], especially in the microwave range.

So far, the Fe_3O_4 nanoparticles have been synthesized in many morphologies, shapes, and sizes to produce a better performance in absorbing microwave. Other strategies have also been conducted to produce the Fe_3O_4 nanoparticles in nanocomposites [4–8], core shells [9-11], or coated with other materials [12,13]. Unfortunately, studies that exploring microscopic phenomena related to the microwave absorption properties of the Fe_3O_4 nanoparticles are rarely reported. Therefore, the study by focusing on the microscopic view of the microwave absorption of the Fe_3O_4 nanoparticles is a great importance, both through the development of theoretical, computational, and experimental research.

Based on the previous studies, the microwave absorption values of the various materials using Fe_3O_4 as the main compound have maximum were in the range of 2-12 GHz [14–16]. From such literature, it is known that the reflection loss tends to increase by decreasing the thickness of the

samples and by increasing frequency. Therefore, it is essential to investigate the microscopic phenomenon regarding microwave absorption of Fe_3O_4 nanoparticles. The importance of this study is not only to reveal fundamental physical phenomena in the material but also to predict and improve microwave absorption performance for further application development. In this paper, we report the symmetry top rotational molecular model and microwave absorption calculation method for the Fe_3O_4 nanoparticles.

2. Materials and methods

In this work, the calculation method was employed by symmetry top rotational molecular model. Based on the crystal structure, Fe_3O_4 is a material consisting of two substructures, i.e., tetrahedral and octahedral structures. The crystal structure of the Fe_3O_4 is visualized in Figure 1. The two substructures have different characters in absorbing electromagnetic wave due to the different inertial moment resulting in the different energy levels of them. The inertial moment for the substructures are represented in Equation 1-3.

$$I_{oct} = 4m_{oxy}\, r_A^2 \tag{1}$$

$$I_{tet//} = 2m_{oxy}(1-\cos\theta)r_B^2 \tag{2}$$

$$I_{tet\perp} = m_{oxy}(1-\cos\theta)r_B^2 + \frac{m_{oxy}}{m_{Fe}+4m_{oxy}}(m_{Fe}+m_{oxy})(1+2\cos\theta)r_B^2 + ((m_{Fe}+3m_{oxy})r_B + \tag{3}$$

$$6m_{oxy}r_B\left(\frac{1}{3}(1+2\cos\theta)\right)^{1/2})r_B$$

where I_{oct} is the inertia moment for octahedral phase of the Fe_3O_4 particle, $I_{tet//}$ and $I_{tet\perp}$ are the inertia moments for tetragonal phase of the Fe_3O_4 particle, m_{oxy} is the mass of oxygen atom (16 amu), m_{Fe} is the mass of an iron atom (55.847 amu), r_A is the distance of oxygen atom to Fe (+3) atom (2.066 Å) in the crystal balance condition [17]. Based on the data, we propose the rotational Hamiltonian of tetrahedral and octahedral for Fe_3O_4 particles as presented in Equation 4-7.
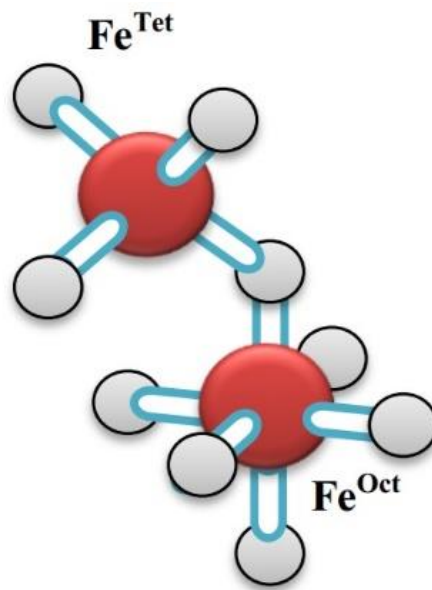

Figure 1. Tetrahedral and octahedral structure of Fe_3O_4 particles

$$H_{okt} = \frac{J^2}{2I_{okt}} \tag{4}$$

$$H_{tet} = \frac{J^2}{2I_{tet\perp}} + (\frac{1}{2I_{tet//}} - \frac{1}{2I_{tet\perp}})J_z^2 \tag{5}$$

where H_{okt} is Hamiltonian for the octahedral phase of the Fe_3O_4 particle and H_{tet} is Hamiltonian for the tetragonal phase of the Fe_3O_4 particle.

If the two Hamiltonian are subjected to Eigenfunction of the Fe_3O_4 particles, the Eigenvalue will be presented in Equation 6-7.

$$H_{okt}|J.K\rangle = \frac{J^2}{2I_{okt}}|J.K\rangle = \frac{J(J+1)\hbar^2}{2I_{okt}}|J.K\rangle \tag{6}$$

$$H_{tet}|J.K\rangle = \frac{J^2}{2I_{tet\perp}}|J.K\rangle + (\frac{1}{2I_{tet//}} - \frac{1}{2I_{tet\perp}})J_z^2|J.K\rangle = \left(\frac{J(J+1)\hbar^2}{2I_{tet\perp}} + (\frac{1}{2I_{tet//}} - \frac{1}{2I_{tet\perp}})K^2\hbar^2 \right)|J.K\rangle \tag{7}$$

where J is quantum number of molecular orbit with the value of 0 to ∞, while $M = J, J-1, \ldots, -J$.

Based on the *Raman selection rules* [18], the rotational transition can be found for $\Delta J = \pm 1, \pm 2$. Therefore, it will imply on the change of allowed energy level as shown in Equation 8.

$$\Delta E_{okt} = \frac{\hbar^2}{2I_{okt}}(2J+1) \text{ or } \Delta E_{okt} = \frac{\hbar^2}{2I_{okt}}(4J+6) \tag{8}$$

The above requirement can also apply to the change of energy level on tetrahedral and octahedral structures of Fe_3O_4 particles. Besides that, in this work, we also apply the rotational energy of Fe_3O_4 particles. Therefore, the visualization of the absorption intensity of the Fe_3O_4 particles depends on the ratio of the number of the particles in the certain level and ground state [19].

$$\frac{N_J}{N_0} = (2J+1)\exp\left(-\frac{E_J}{k_B T}\right) \tag{9}$$

where J is total orbital quantum number, N_J is molecular number on J-level, N_0 is molecular number on ground state, E_J is rotational energy level, and T is temperature when the photons directed to the samples.

Using Raman selection rule, we calculate and visualize the absorption of the electromagnetic intensity of Fe_3O_4 particles as a function of frequency using Borland Delphi 7. The primary technique for the calculation is by determining the change of energy level of the Fe_3O_4 particles using Equation 8 and conducting similarity with the Einstein's photon energy ($E = hf$). Based on the calculated frequency, we interpolate for all frequencies of the electromagnetic wave that suitable with the absorbed photon intensity as shown in Equation 9.

3. Results and discussion

Based on the theory of quantum theory, the intensity of the absorbed photon is proportional to the square of the transition moment represented by Equation 10.

$$R_r = \int \psi_r^* \mu \psi_r'' d\tau \tag{10}$$

Where ψ_r'' and ψ_r^* are two functions of the state of the system in which the molecular transition occurs [20]. For the rotational system, the transition moment of the system is proportional to the number of molecules at that level [19], where the formulation is given by Equation 9.

According to the above calculations, the visualization of microwave absorption by Fe_3O_4 particles is obtained as the curve in Figure 2. Based on the curve, it is seen that the intensity of the photon

absorbed by the Fe_3O_4 particles increases with the increase of the quantum number of molecular orbitals J. The frequency characteristics of the photons absorbed by Fe_3O_4 particles ranging in the range of 2-12 GHz. It is intuitively understood that the above visualization of the theoretical results is in accordance with the result of microwave absorption characters for the samples with the main materials of Fe_3O_4 particles. It is due to the suitability of the absorption curve obtained from the characterization and theoretical visualization. In addition, the microwave absorption characters for the sample with the thickness variation obtained a curve that is not different from the expectation, i.e., the maximum absorption occurs at a frequency of about 10 GHz as shown in Figure 3 [21].
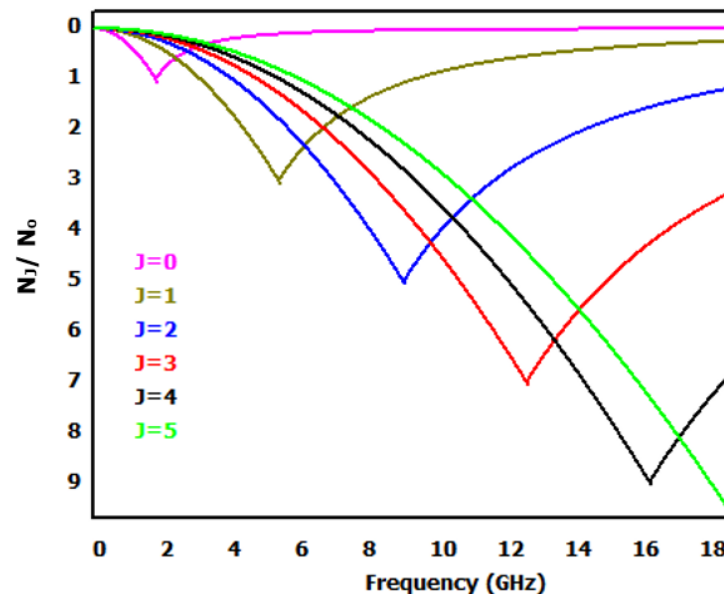

Figure 2. Visualization of ratio of molecule number and frequency of absorbed photon

Physically, the absorption of electromagnetic waves of the materials including Fe_3O_4 particles has a close relationship with the optical quantum phenomenon that is the phenomenon of stimulation absorption. If a photon comes to a molecule at a particular energy level, a jumping of the molecular energy level from low energy to higher energy can occur as long as its frequency is proportional to the difference between the two energy levels of the molecule. This jumping energy must be accompanied by photon absorption events [20]. Schematically, the absorption event is illustrated in Figure 4.

Drude Lorentz's theory has described the complex permittivity as one of the causes of electromagnetic wave absorption [22]. Thus, it can be concluded that the reflection loss value obtained from the permittivity complex and permeability complex [23], is proportional to the intensity of photons absorbed by the material. Therefore, the visualization curve of the rotational transition, which is a theoretical model, the intensity of photons absorbed by Fe_3O_4 particles can be compared to the reflection loss curve of the experiment.
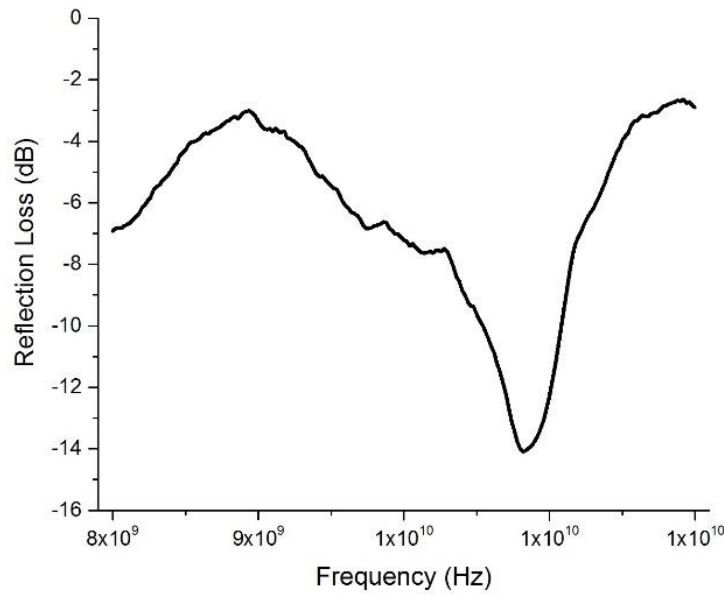
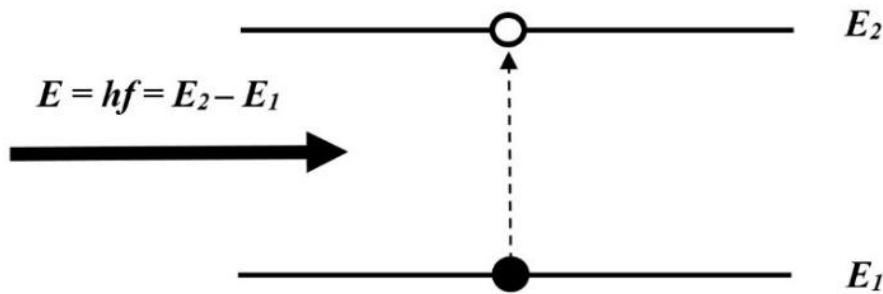**Figure 3.** The reflection loss of the prepared Fe_3O_4 nanoparticles

Figure 4. Schematic of two energy levels of particle population stimulated by photon

From the characterization of microwave absorption properties of the material, it can be seen that the thickness of the sample causes a change in the level of frequency of absorbed electromagnetic waves. The thicker the sample layer, the lower the absorbed electromagnetic wave frequency. This phenomenon is based on the physics concept for single-layer absorber as shown in Equation 11-12 [23]:

$$RL(dB) = 20Log \left| \frac{Z_{in} - 1}{Z_{in} + 1} \right| \tag{11}$$

Where RL and Z_{in} are the reflection loss and input impedance, respectively.

$$Z_{in} = \left(\frac{\mu_r}{\varepsilon_r} \right)^{\frac{1}{2}} \tanh \left[j \left(\frac{2\pi fd}{c} \right) (\mu_r \varepsilon_r)^{\frac{1}{2}} \right] \tag{12}$$

Where ε_r is the complex permittivity of the sample, f is the frequency, d is the thickness of the sample, and c is the speed of light in vacuum.

Based on the theoretical visualization of the rotational model of the molecule, the frequency and intensity of electromagnetic waves absorbed by the Fe_3O_4 particles depend on the quantum number of

molecular orbitals *J*, where the higher the quantum number of the molecular orbital, the higher the absorbed intensity [24]. It can be understood by referring the equations that become the basis of the visualization, Equation 8-9. From the experimental data and theoretical model, there is a similarity of characteristics related to the shape of the curve. This phenomenon related to the quantum number of molecular orbitals J in quantum mechanics is a quantum number that describes the shape of a molecular orbit. When samples have different thicknesses, the attractive forces experienced by atoms in the molecule are also different. Thus, the shape of the orbit of atoms in the molecule changes implying a change in the quantum number of molecular orbitals *J*. The reasoning that causes the difference in sample thickness affects the peak frequency shift for reflection loss.

4. Conclusions

Based on the calculation and visualization of the absorbed electromagnetic intensity by Fe_3O_4 particles via rotational molecular transition approach, it is identified that the absorption pattern of the Fe_3O_4 particles has a similar pattern with the experimental data. It also gives information that the mechanism occurs at the electromagnetic absorption of the Fe_3O_4 particles is the rotational molecular mechanism. Therefore, for further experiment, the rotational molecular mechanism can be taken into account for investigating microwave absorption, especially for the Fe_3O_4 particles.

Acknowledgments

References

[1] Li Y, Chen G, Li Q, Qiu G and Liu X 2011 Facile synthesis, magnetic and microwave absorption properties of Fe_3O_4/polypyrrole core/shell nanocomposite *J. Alloys Compd.* **509** 4104–7.

[2] Wang Y, Li T, Zhao L, Hu Z and Gu Y 2011 Research Progress on Nanostructured Radar Absorbing Materials *Energy Power Eng.* **03** 580–4.

[3] Shi L, Zhao Y, Li Y, Han X and Zhang T 2017 Octahedron Fe_3O_4 particles supported on 3D MWCNT/graphene foam: In-situ method and application as a comprehensive microwave absorption material *Appl. Surf. Sci.* **416** 329–37.

[4] Hou C, Li T, Zhao T, Liu H, Liu L and Zhang W 2013 Electromagnetic wave absorbing properties of multi-wall carbon nanotube/ Fe_3O_4 hybrid materials *New Carbon Mater.* **28** 184–90.

[5] Cao J, Fu W, Yang H, Yu Q, Zhang Y, Wang S, Zhao H, Sui Y, Zhou X, Zhao W, Leng Y, Zhao H, Chen H and Qi X 2010 Fabrication, characterization and application in electromagnetic wave absorption of flower-like ZnO/ Fe_3O_4 nanocomposites *Mater. Sci. Eng. B* **175** 56–9.

[6] Amir M, Güner S, Yıldız A and Baykal A 2017 Magneto-optical and catalytic properties of Fe_3O_4@HA@Ag magnetic nanocomposite *J. Magn. Magn. Mater.* **421** 462–71.

[7] Bera R, Das A K, Maitra A, Paria S, Karan S K and Khatua B B 2017 Salt leached viable porous Fe_3O_4 decorated polyaniline–SWCNH/PVDF composite spectacles as an admirable electromagnetic shielding efficiency in extended Ku-band region *Compos. Part B Eng.* **129** 210–20.

[8] Li S, Zhou Z, Zhang T, Jiang G and Su R 2014 Synthesis and characterization of Ag/Fe_3O_4 electromagnetic shielding particles *J. Magn. Magn. Mater.* **358**–**359** 27–31.

[9] Khani O, Shoushtari M Z, Jazirehpour M and Shams M H 2016 Effect of carbon shell thickness on the microwave absorption of magnetite-carbon core-shell nanoparticles *Ceram. Int.* **42** 14548–56.

[10]   Chen Y-J, Xiao G, Wang T-S, Ouyang Q-Y, Qi L-H, Ma Y, Gao P, Zhu C-L, Cao M-S and Jin H-B 2011 Porous Fe_3O_4/Carbon Core/Shell Nanorods: Synthesis and Electromagnetic Properties *J. Phys. Chem. C* **115** 13603–8.

[11]   Chen Y-J, Zhang F, Zhao G, Fang X, Jin H-B, Gao P, Zhu C-L, Cao M-S and Xiao G 2010 Synthesis, Multi-Nonlinear Dielectric Resonance, and Excellent Electromagnetic Absorption Characteristics of Fe_3O_4/ZnO Core/Shell Nanorods *J. Phys. Chem. C* **114** 9239–44.

[12]   Qiang C, Xu J, Zhang Z, Tian L, Xiao S, Liu Y and Xu P 2010 Magnetic properties and microwave absorption properties of carbon fibers coated by Fe_3O_4 nanoparticles *J. Alloys Compd.* **506** 93–7

[13]   Meng X, Wan Y, Li Q, Wang J and Luo H 2011 The electrochemical preparation and microwave absorption properties of magnetic carbon fibers coated with Fe_3O_4 films *Appl. Surf. Sci.* **257** 10808–14.

[14]   Chu H, Zeng Q, Chen P, Yu Q, Xu D, Xiong X and Wang Q 2017 Synthesis and electromagnetic wave absorption properties of matrimony vine-like iron oxide/reduced graphene oxide prepared by a facile method *J. Alloys Compd.* **719** 296–307.

[15]   Liu X, Cao K, Chen Y, Ma Y, Zhang Q, Zeng D, Liu X, Wang L-S and Peng D-L 2017 Shape-dependent magnetic and microwave absorption properties of iron oxide nanocrystals *Mater. Chem. Phys.* **192** 339–48.

[16]   Zheng Y, Wang X, Wei S, Zhang B, Yu M, Zhao W and Liu J 2017 Fabrication of porous graphene- Fe_3O_4 hybrid composites with outstanding microwave absorption performance *Compos. Part Appl. Sci. Manuf.* **95** 237–47.

[17]   Friák M, Schindlmayr A and Scheffler M 2007 *Ab initio* study of the half-metal to metal transition in strained magnetite *New J. Phys.* **9** 5–5.

[18]   Atkins P W and Friedman R 2011 *Molecular quantum mechanics* (Oxford ; New York: Oxford University Press).

[19]   Hollas J M 2004 *Modern spectroscopy* (Chichester ; Hoboken, NJ: J. Wiley).

[20]   Fox M 2006 *Quantum optics: an introduction* (Oxford ; New York: Oxford University Press).

[21]   Taufiq A, Bahtiar S, Sunaryono, Hidayat N, Hidayat A, Mufti N, Diantoro M, Fuad A, Munasir, Rahmawati R, Adi W A, Pratapa S and Darminto 2017 Preparation of Superparamagnetic $Zn_{0.5}Mn_{0.5}Fe_2O_4$ Particle by Coprecipitation-Sonochemical Method for Radar Absorbing Material *IOP Conf. Ser. Mater. Sci. Eng.* **202** 012024.

[22]   Moliton A 2007 *Basic electromagnetism and materials* (New York, NY: Springer).

[23]   Che R C, Peng L-M, Duan X F, Chen Q and Liang X L 2004 Microwave Absorption Enhancement and Complex Permittivity and Permeability of Fe Encapsulated within Carbon Nanotubes *Adv. Mater.* **16** 401–5.

[24]   Alexander A J, Kroto H W and Walton D R M 1976 The microwave spectrum, substitution structure and dipole moment of cyanobutadiyne, HCCCCCN *J. Mol. Spectrosc.* **62** 175–80.